Gelatin—Hyaluronic Acid Hydrogels with Tuned Stiffness to Counterbalance Cellular Forces and Promote Cell Differentiation

Sara Poveda-Reyes, Vladimira Moulisova, Esther Sanmartín-Masiá, Luis Quintanilla-Sierra, Manuel Salmerón-Sánchez,* Gloria Gallego Ferrer*

Cells interact mechanically with their environment, exerting mechanical forces that probe the extracellular matrix (ECM). The mechanical properties of the ECM determine cell behavior and control cell differentiation both in 2D and 3D environments. Gelatin (Gel) is a soft hydrogel into which cells can be embedded. This study shows significant 3D Gel shrinking due to the high traction cellular forces exerted by the cells on the matrix, which prevents cell differentiation. To modulate this process, Gel with hyaluronic acid (HA) has been combined in an injectable crosslinked hydrogel with controlled Gel–HA ratio. HA increases matrix stiffness. The addition of small amounts of HA leads to a significant reduction in hydrogel shrinking after cell encapsulation (C2C12 myoblasts). We show that hydrogel stiffness counterbalanced traction forces of cells and this was decisive in promoting cell differentiation and myotube formation of C2C12 encapsulated in the hybrid hydrogels.

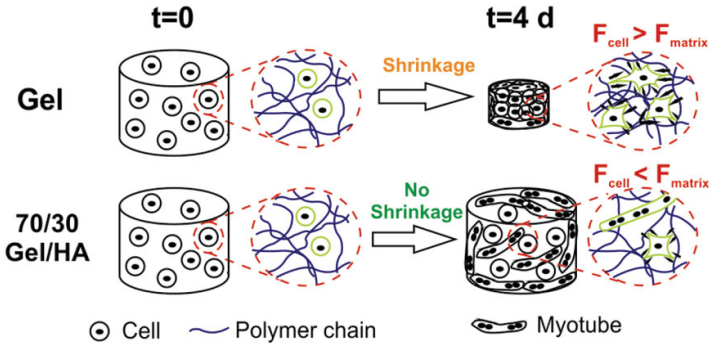

Dr. S. Poveda-Reyes, E. Sanmartín-Masiá, Prof. G. Gallego Ferrer
Center for Biomaterials and Tissue Engineering (CBIT)
Universitat Politècnica de València
Valencia 46022, Spain
E-mail: ggallego@ter.upv.es
Dr. V. Moulisova, Prof. M. Salmerón-Sánchez
Division of Biomedical Engineering
School of Engineering
University of Glasgow
Glasgow G12 8QQ, UK
E-mail: Manuel.Salmeron-Sanchez@glasgow.ac.uk
Prof. L. Quintanilla-Sierra
BIOFORGE Group, Centro de Investigación Científica y Desarrollo Tecnológico
Campus de Miguel Delibes
Universidad de Valladolid
Valladolid 47011, Spain
Prof. L. Quintanilla-Sierra, Prof. G. Gallego Ferrer
Biomedical Research Networking Center in Bioengineering Biomaterials and Nanomedicine (CIBER-BBN)
Valencia 46022, Spain

1. Introduction

Hydrogels have been widely studied as artificial extracellular matrices (ECMs) capable of mimicking the ECM of different tissues due to their high water retention capability, permeability to cell nutrients and metabolites, and good mechanical properties and biocompatibility.[1] ECM is mainly composed of water, fibrous proteins (e.g., collagens, elastins, fibronectins and laminins), and proteoglycans (e.g., hyaluronic acid (HA), perlecan, decorin, etc.) with a composition and topology that depend on the specific tissue or cell population.[2] Ideally, materials for tissue engineering should mimic the native ECM and allow cell adhesion, proliferation, differentiation, and synthesis of a new ECM with the same characteristics as the native one. This includes not only hydration and mechanical properties but also adhesion cues should be provided to enable appropriate cell–material interactions. For this, nonadhesive hydrogels are usually combined with peptide

DOI: 10.1002/mabi.201500469

ligands able to promote integrin-mediated adhesion.[3] Injectable hydrogels also allow the encapsulation of cells and bioactive molecules on the site of the defect, overcoming the problem of cell diffusion in the injection site and enabling the sustained release of bioactive cues.[3d]

Most hydrogels need to be crosslinked in order to avoid dissolution at body temperature. The usual crosslinking methods are chemical reactions or photoinduced processes.[4] Most chemical crosslinking reactions are cytotoxic and leave behind solvents, initiators or unreacted substances that often produce inflammation and cell death.[5] These hydrogels are thus preformed in the lab and thoroughly washed to remove undesired reactants prior to their clinical application. Photocrosslinked hydrogels have additional drawbacks, since the monomer solution limits light penetration and some can change their transparency as the reaction progresses, diminishing hydrogel homogeneity.[3e] Noncytotoxic enzyme-mediated crosslinking reactions have recently been proposed as an alternative. These have the added advantage of enabling the gel and cells to be injected at the site of the tissue defect.[6] The desirable characteristics of an injectable hydrogel are: (i) fast and controlled crosslinking to keep cells within the injection site, able to adjust its shape to the defect and avoid its mechanical failure; (ii) cell adhesive sequences to promote cell adhesion and differentiation; and (iii) sufficient mechanical stability to act as a temporary scaffold while the cells produce their own ECM and form new tissue.

Skeletal muscle cells have been proposed as a good cell model to study the influence of hydrogel composition and stiffness on cell behavior, since their phenotype clearly changes from undifferentiated myoblasts to differentiated myocytes forming myotubes in short culture times.[7] Many studies have focused on the factors that influence myoblast differentiation; incorporation of adhesion sequences such as RGD,[3a] the increase in matrix stiffness,[8] polymer conductivity,[9] high cell seeding densities,[3c] co-cultures of myoblasts with fibroblasts[10] or neural cells,[11] or the use of micropatterns to guide myotube formation,[3e,12] have been reported to improve myoblast adhesion and differentiation into myotubes.

Rowley et al. first reported the differentiation of skeletal myoblasts on a substrate without providing whole ECM molecules (e.g., fibronectin or collagen) using alginate modified with the GGGGRGDY peptide, proving that myoblast proliferation and differentiation improved with higher RGD density and higher guluronic acid content in alginate composition.[3a] Yeo et al. used a photocrosslinkable chitosan/acryloyl-poly(ethylene glycol)-RGDS hydrogel at a concentration of 5×10^{-3} M RGD. The myoblasts remained rounded and showed a lack of adhesion in chitosan, as usually happens in other noncell adhesive hydrogels. The authors demonstrated that the incorporation of the RGD sequence promoted cell attachment, proliferation and differentiation for up to 13 d of cell culture.[3d] RGD has also been incorporated into enzymatic crosslinked hydrogels. Jun et al. demonstrated that the adhesion peptide GRGDGGGGGY can successfully be incorporated into tetronic–tyramine crosslinked materials catalyzed by horseradish peroxidase (HRP) and H_2O_2 initiators, regulating cell adhesion, formation of focal adhesions and myoblast differentiation.[6d]

Other factors that regulate myoblast behavior are the cell seeding density and material stiffness or contractility. Salimath et al. showed that the highest cell survival was obtained at cell seeding values of $4—8 \times 10^6$ cells mL^{-1} in an poly(ethylene glycol)-maleimide (PEG-MAL) hydrogel functionalized with the RGD sequence, due to the formation of cell–cell interactions and the equilibrium between the number of cells and nutrient availability.[3c] Gupta et al. studied the effect of stiffness and wettability on poly(vinyl alcohol) hydrogels and concluded that this type of hydrogel provides better myoblast attachment and proliferation with increased stiffness and polymer hydrophobicity.[8] Other approaches to improving cell growth and differentiation include the formation of hydrogels with electrical conductive nanotubes[13] or the quite recent use of conducting polymer hydrogels,[9] which have electrical properties that enhance muscle and nerve cell growth.

In this study we present a family of injectable hydrogels that mimic the composition of the ECM, with a homogeneous distribution of gelatin (Gel) and HA chains by enzymatic gelation of aqueous solutions of different mixtures of both polymers. We hypothesized that this combination would better promote the differentiation of encapsulated cells than pure hydrogels, due to the synergistic benefits of both components. Gel provides the protein character and has more available RGD adhesion sequences than collagen,[14] HA provides resilience and hydrodynamic properties. Similar injectable hybrid hydrogels have been previously reported, as for example by UV light crosslinking methacrylate precursor mixtures[15] or by reacting thiol functionalized precursor mixtures with polyethylene diacrylate.[16] Despite the fact that the concept of combining Gel and HA to obtain ECM inspired hydrogels is not new, this is the first time that tyramine derivatives of both components have been combined. Hydrogels were optimized as regards their miscibility by using low molecular weight HA, since high molecular weight HA solutions are too viscous to mix easily with Gel solutions. Swelling and mechanical studies were performed to demonstrate the hydration and reinforcement effects provided by HA in the different Gel-HA hydrogels. C2C12 murine myoblasts were embedded in the different hydrogels and myoblast differentiation was correlated with matrix composition and contractility. To our

knowledge this is the first time that these enzymatically gellable hydrogel mixtures have been proposed to induce cell differentiation. Our results confirm that these matrices are promising candidates for soft tissue engineering.

2. Experimental Section

2.1. Materials

HA sodium salt from *Streptococcus equi*, Gel from porcine skin (gel strength 300, Type A), tyramine hydrochloride (98%), peroxidase from horseradish Type VI (HRP), hydrogen peroxide solution (30% w/w in H_2O, with stabilizer), *N*-Hydroxysuccinimide (98%, NHS), Dulbecco's phosphate buffered saline (DPBS), 2-(*N*-Morpholino)ethanesulfonic acid (>99%, MES), sodium azide (>99.5%, ReagentPlus), 4-(2-hydroxyethyl)piperazine-1-ethanesulphonic acid (HEPES), potassium chloride (for molecular biology), and dialysis tubing (3500 and 12400 MWCO) were purchased by Sigma-Aldrich (USA). *N*-(3-Dimethylaminopropyl)-*N*′-ethylcarbodiimide hydrochloride (EDC) was supplied by Iris Biotech GmbH (Germany). Sodium chloride (synthesis grade) and potassium dihydrogen phosphate (extra pure) were from Scharlab (Spain).

For cell culture experiments, C2C12 cells, primary antibody for myosin (MF-20b, 800 μg mL^{-1}) was from Developmental Studies Hybridoma Bank (DSHB, USA) and secondary antibody rabbit anti-mouse Cy3 was purchased from Jackson Immunoresearch (USA). Mounting reagent Vectashield with DAPI (4,6-diamidino-2-phenylindole) was from Vector Laboratories Inc (USA). Goat serum, trypsin/EDTA, P/S and Triton X-100, 37% formaldehyde were from Sigma-Aldrich (USA). FBS, DMEM with high glucose and ITS-X were purchased from Gibco and NucBlue was from Molecular Probes (ThermoFisher Scientific, USA). BODIPY FL Phallacidin was obtained from Life Technologies (USA) and OCT compound mounting medium for cryotomy was purchased from VWR (USA).

Calcium Free Krebs Ringer Buffer (CF-KRB) solution was prepared with 115×10^{-3} M sodium chloride, 5×10^{-3} M potassium chloride, 1×10^{-3} M potassiumdihydrogen phosphate, and 25×10^{-3} M HEPES.

2.2. Gelatin and Hyaluronic Acid Tyramine Grafting

The basic materials (Gel and HA) were grafted with tyramine in order to obtain hydrogels capable of being formed by enzymatic crosslinking in situ. The molar ratios used to obtain both type of materials are shown in Table 1.

For Gel, 2% (wt/vol) Gel in 50×10^{-3} M MES was dissolved at 60 °C for 30 min under stirring (0.4 g of Gel and 0.195 g of MES in 20 mL miliQ water). Then 0.111 g of tyramine hydrochloride was added and the mixture was stirred for 20 min at room temperature. The pH was adjusted to 6 and 7 mg of NHS was added and stirred for 30 min for homogenization. 123 mg of EDC was then added and the mixture was stirred for another 24 h at 37 °C. Unreacted reagents were removed via dialysis against deionized water for 48 h (with a dialysis tube of 12400 MWCO). Finally, the modified Gel was lyophilized in a LyoQuest (Telstar Life Science Solutions, Japan) for further use. No precipitation of self-crosslinked Gel was observed during tyramine grafting. EDC activates the carboxylic acid residues of aspartic and glutamic acids in Gel that could react with the free amine groups of lysine in Gel producing Gel auto-crosslinking.[17] However, in the presence of tyramine, activated carboxylic groups of Gel would preferentially react with the free amine groups of tyramine as they have less steric hindrance than the amines of Gel. If Gel intra- and intermolecular bonds would be abundant the resulting Gel–Tyr would not be soluble in water, which was not the case.

For the HA tyramine grafting, first, HA of low molecular weight (around 320 000 Da) was obtained from acid degradation of the high molecular weight HA.[18] Briefly, 500 mg of high molecular weight HA were dissolved in 500 mL of HCl at pH 0.5, and the solution was stirred for 24 h at 37 °C for HA degradation. The reaction was stopped by adjusting the pH to 7 with 1 N NaOH. The obtained solution was dialyzed (with a dialysis tube of 3500 MWCO) against distilled water for 4 d and then lyophilized to dry it. For the tyramine grafting, 100 mg HA (0.5% wt/vol) was then dissolved in 20 mL 150×10^{-3} M NaCl with 1.08 g MES and 75×10^{-3} M NaOH (pH 5.75). 86.54 g of tyramine hydrochloride was added and the solution was stirred until full dissolution. The pH was adjusted at 5.75 and 47.77 mg EDC and 2.87 mg NHS were added. The obtained solution was stirred for 24 h in order to obtain the tyramine grafting and was then dialyzed (dialysis tube of 3500 MWCO) 24 h with 150×10^{-3} M NaCl and another 24 h against deionized water, changing the dialysis solution three times daily. Finally, the tyramine grafted HA solution was lyophilized for further use.

To determine the quantity of phenol groups due to the grafting of tyramine (Tyr) in Gel and HA polymeric chains, the absorbance of 0.1% wt/wt aqueous solution of grafted Gel and HA was measured at 275 nm with the CECIL CE9200 UV/VIS double beam spectrophotometer (Buck Scientific, Norwalk, USA), obtaining values of 1.9×10^{-7} mol Tyr mg^{-1} Gel and 9.69×10^{-8} mol Tyr mg^{-1} HA, for tyramine grafted Gel and HA respectively. The content of introduced phenol groups was calculated from a calibration curve of known percentages of tyramine hydrochloride in distilled water. Tyramine grafting onto the Gel and HA chains was also studied by ^{1}H-NMR (see supplementary data). The degree of substitution of HA–Tyr (the number of tyramine molecules per 100 repeating units) was calculated by comparing the ratio of the relative peak integrations of the phenyl protons of tyramine (peaks at 7.2 and 6.9 ppm) and the methyl protons of HA (1.9 ppm) (see supplementary data), obtaining a degree of substitution of 7%. For the modified Gel, its NMR spectrum shows the presence of distinctive

Table 1. Molar ratios used in the gelatin–tyramine and hyaluronic-acid–tyramine coupling reaction.

	EDC/COOH	EDC/Tyramine	NHS/EDC	Tyramine/COOH
Gelatin	2:1	1:1	1:10	2:1
Hyaluronic acid	1:1	1:2	1:10	2:1

peaks for both pairs of aromatic ring protons at 7.0 and 6.7 ppm, what indicates that the grafting has been successful. However, the degree of grafting cannot be obtained using this method since the percentage of the characteristic amino acids that form its structure is not known. Therefore, there is not a reference peak that can be used for the integration and the calculation of the grafting degree. Degree of substitution of GEL–Tyr was then calculated with the results of UV spectrophotometry. Taking into account that type A Gel with gel strength 300 has 80 mmol of COOH per 100 g of Gel (data provided by the supplier), a grafting of 1.9×10^{-7} mol Tyr mg^{-1} Gel corresponds to a degree of substitution of 24% (number of tyramine molecules per 100 COOH molecules). Degree of substitution corresponds to the yield of tyramine coupling with both GEL and HA, as the molar ratios of EDC and tryamine used in the reactive mixture (Table 1) are sufficient to activate all their COOH groups.

2.3. Gel/HA Hydrogels Preparation

Hydrogels were obtained with different proportions of Gel/HA tyramine derivatives (100/0, 70/30, 50/50, 30/70, and 0/100 vol/vol). First, 2% wt/vol Gel and 2% wt/vol HA solutions in CF-KRB were prepared at 37 °C. For complete dissolution, HA solution was maintained at 4 °C for 24 h and Gel solution was heated at 37 °C for 30 min. Hydrogels of 300 μL were obtained mixing 80 vol% of the Gel/HA mixture in different proportions, 10 vol% of 12.5 U mL^{-1} HRP (1.25 U mL^{-1} in the final volume) and 20×10^{-3} M H_2O_2 (2×10^{-3} M in the final volume). The enzymatic reaction was achieved after 9 min, accurate measurement of gelation time of the different samples was determined by rheology as explained in the next section. The samples were kept in DPBS with 0.02% wt/vol sodium azide to prevent bacterial growth in a refrigerator for further characterization. Complete incorporation of soluble Gel and HA chains in the different hydrogel networks was assumed as the UV spectra of the storage DPBS buffers were identical to the spectrum of fresh DPBS (results not shown).

2.4. Characterization of Gelation Process by Rheology

Rheological experiments were performed on a strain-controlled AR-2000ex rheometer (TA Instruments). A solvent trap geometry of parallel plates (made of nonporous stainless steel, diameter = 20 mm) was used to reduce solvent loss during the experiment. The gap between the plates was around 1200 μm. Sample temperature was controlled and maintained by a Peltier device and measurements were always carried out at 37 °C. Measurements were made in a shear deformation mode. An oscillatory time sweep was selected to follow the gelation dynamics of the samples. The mixtures of Gel, HA and enzyme were arranged on the plate at 37 °C. After adding the correct amount of H_2O_2 to initiate the reaction, measurements were recorded (after the 10–15 s required to lower the plate). The time evolution of the rheological parameters was recorded for a period of 20 min. Strain and frequency were selected at 1% and 1 Hz, respectively.

2.5. Scanning Electron Microscopy

Cross sections of the different Gel/HA compositions were obtained by lyophilizing the swollen samples and cutting them with a sharp blade. For lyophilization, swollen samples were frozen in liquid nitrogen and stored overnight at −80 °C. Then, frozen samples were placed in the lyophilizer, preconditioned at −80 °C, to sublimate the water in them. The sample sections were then mounted on adhesive carbon black, sputter-coated with gold and examined at an accelerating voltage of 10 kV and 15 mm working distance with a scanning electron microscope (SEM; JEOL JSM-5410, Japan). ImageJ software was used to obtain the pore size from the analysis of the images.

2.6. Gel/HA Equilibrium Water Content

Gel/HA hydrogels were prepared in cylindrical molds with a diameter of 8 mm and 300 μL. After crosslinking, they were immersed in DPBS with 0.02% wt/vol sodium azide solution at 37 °C overnight to reach equilibrium and weighed (m_w), this will be the equilibrium water absorption value). Afterward, the samples were rinsed twice with water to remove the DPBS, and finally lyophilized to obtain the dry mass of the sample (m_d). The equilibrium water content (EWC) was obtained using Equation (1)

$$\mathrm{EWC}(\%) = \frac{m_w - m_d}{m_d} \times 100 \tag{1}$$

The volumetric swelling ratio (Q_v) was estimated using Equation (2)

$$Q_v = \frac{\dfrac{\mathrm{EWC}}{100 \cdot \rho_w} + \dfrac{1}{\rho_{\mathrm{polymer}}}}{\dfrac{1}{\rho_{\mathrm{polymer}}}} \tag{2}$$

considering that the density of the solvent (DPBS) is the density of water (ρ_w). For pure hydrogels a density of dry polymer (ρ_{polymer}) of 1.44 g cm^{-3}[19] and 1.229 g cm^{-3}[20] were used for the Gel and HA, respectively. Ideal behavior was assumed to estimate the density of the mixtures, calculating their specific volumes by using the specific volume and mass fraction of pure samples.

2.7. Gel/HA Unconfined Compression Assay

Five replicates of each composition were tested in unconfined compression at room temperature on a Thermomechanical Analysis device (TMA/ss6000, Seiko Instruments Inc, Japan) immersed in DPBS. First, a 2% predeformation was applied to the hydrogels and then the samples were tested at a rate of 50 μm min^{-1} until 90% strain. Young's modulus was obtained for each composition from the slope in the first linear region (up to 20% strain).

2.8. Hydrogel Formation for Cell Culture Experiments

2% wt/vol Gel and 2% wt/vol HA solutions were prepared by dissolving the lyophilized powder in DMEM with 1% P/S, 24 h at 4 °C for HA and 30 min at 37 °C for Gel. 12.5 U mL^{-1} HRP solution was then added to the prepared solutions at a volume ratio of 10/80 (mL of HRP solution/mL Gel or HA solution) and the obtained mixture was filtered through a 0.22 μm syringe filter under the

cell culture hood for sterilization. Solutions of different proportions (100/0, 70/30, 50/50, 30/70, 0/100 vol%/vol%) of Gel+HRP and HA+HRP were then prepared. Cells were then added to each Gel/HA mixture. Finally, 45 μL of the Gel/HA cell suspension were crosslinked with 5 μL of 20×10^{-3} M H_2O_2 on each well of the cell culture plate.

2.9. Myosin Differentiation

C2C12 myoblasts were expanded in Dulbecco's Modified Eagle Medium (DMEM) with 20% FBS and 1% P/S (growth medium), at 37 °C and 5% CO_2 in an incubator. At 60% confluence, cells were released from the culture flask with 4 mL of trypsin/EDTA for 10 s, the trypsin was removed and the flask was incubated for 3 min. 10 mL of growth medium were added to stop trypsin activity, and centrifuged at 1400 rpm for 4 min. Cells were resuspended in DMEM with 1% P/S, counted, the required quantity for each Gel/HA solution was taken, centrifuged at 1400 rpm for 2 min and resuspended in the Gel/HA with HRP solution at a cell density of 8×10^6 cells mL^{-1} (400 000 cells per hydrogel, passage 3). The Gel/HA cell suspension was crosslinked as described above and left in the incubator at 37 °C and 5% CO_2 for 30 min and then cultured in DMEM with 1% ITS and 1% P/S. Triplicates of each composition were produced. Cell medium was changed every 2 d.

After 4 d, samples were washed with DPBS, fixed with 4% formaldehyde for 15 min and washed again with DPBS. For 3D images, samples were permeabilized with 0.1% Triton X-100 in PBS for 20 min at room temperature, washed with PBS, blocked with 5% Goat Serum in PBS (blocking buffer) for 1 h and washed with PBS. Then 1:250 of the primary antibody MF-20 was added in blocking buffer for sarcomeric myosin staining for 1 h, washed with PBS and 1:200 of rabbit antimouse Cy3 secondary antibody in blocking buffer was added for 1 h, washed, and kept in PBS. Images were taken in the fluorescent microscope Zeiss Observer Z1_AX10 at different heights, and the 3D image was taken as *z* projection of the images at the different heights using ImageJ.

Hydrogels were sectioned to obtain better quality fluorescent pictures with less background than 3D images. For this, formaldehyde fixed samples were soaked in 30% wt/vol sucrose in DPBS overnight, included in OCT, frozen with liquid nitrogen, and kept in at −80 °C. Finally, samples were cut at 40 μm with the cryostat Leica CM 1860 UV. Sections were similarly stained, but after adding the secondary antibody the sample was stained with BODIPY FL Phallacidin 1:100 for 20 min, washed and mounted in Vectashield with DAPI. CellC software was used for cell counting. Percentage of differentiation was also calculated with CellC software for five different images of the same sample, having three samples for each composition. This software allows the detection of the quantity of nuclei that are within the area stained for myosin. The percentage of differentiation was obtained as the ratio between the nuclei within the myosin stained area and the total amount of nuclei. Percentage of differentiation is expressed as the mean ± standard deviation.

2.10. Cell Contractility Inhibition

C2C12 cells were cultured in 100/0 Gel/HA and 70/30 Gel/HA hydrogels as described in Section 2.7. Differentiation medium (DMEM with 1% ITS and 1% P/S) was used as culture medium for 3 h and then changed for differentiation medium (DM) with 10×10^{-6} M blebbistatin, which acts as a contractility inhibitor, (DM+BL) for 4 d. Triplicates for each composition of the 100/0 and 70/30 Gel/HA hydrogels were cultured in this medium (3 h in DM and 4 d in DM+BL) and in DM as control. The medium was changed every 2 d.

Immunofluorescence of the samples was carried out as described in Section 2.7. Differences in hydrogel diameter were measured and the shrinkage was calculated according to Equation (3):

$$\text{Shrinkage}(\%) = \frac{\varphi_o - \varphi_f}{\varphi_o} \times 100 \quad (3)$$

where φ_o is the initial diameter and φ_f is the diameter after 4 d of culture.

2.11. Statistical Analysis

For statistical purposes, five replicates of each sample were used for the EWC and compression assays and three replicates were used for the cell culture experiments. The Mann–Whitney (Wilcoxon) test was used to obtain significant differences between groups ($p < 0.05$ was considered significant). Data are given as average ± standard deviation.

3. Results and Discussion

Gel and HA chains were modified by grafting their carboxylic groups with the tyramine amine group using EDC and NHS as reaction catalyzers (see Figure 1). Gel and HA crosslinked hydrogels were obtained by covalently bonding the tyramine groups of the grafted polymers using HRP and H_2O_2 (see Figure 2b). H_2O_2 acts as the oxidant of the tyramine molecule, and the HRP catalyzes the crosslinking reaction, oxidizing two tyramine molecules every crosslinking cycle.[21]

Different Gel/HA compositions (100/0, 70/30, 50/50, 30/70, and 0/100) were synthesized in order to study the combined effect of having more RGD sequences due to the Gel component and higher mechanical stability by having more HA.[22] Figure 2a shows the different Gel/HA hydrogels used for cell differentiation studies. The pictures correspond to 50 μL hydrogels with encapsulated cells just after their crosslinking and prior to add the cell culture medium, so they are not swollen in equilibrium and that is why they appear to be similar in size.

Gelation dynamics was characterized by rheology by performing crosslinking reaction in the plates of the equipment. The storage modulus (G′) of the samples with reaction time is shown in Figure 3. The loss modulus did not show any changes in these tests (it remained constant with a value around 1 Pa, regardless of the hybrid gel composition, results not shown). The reaction was

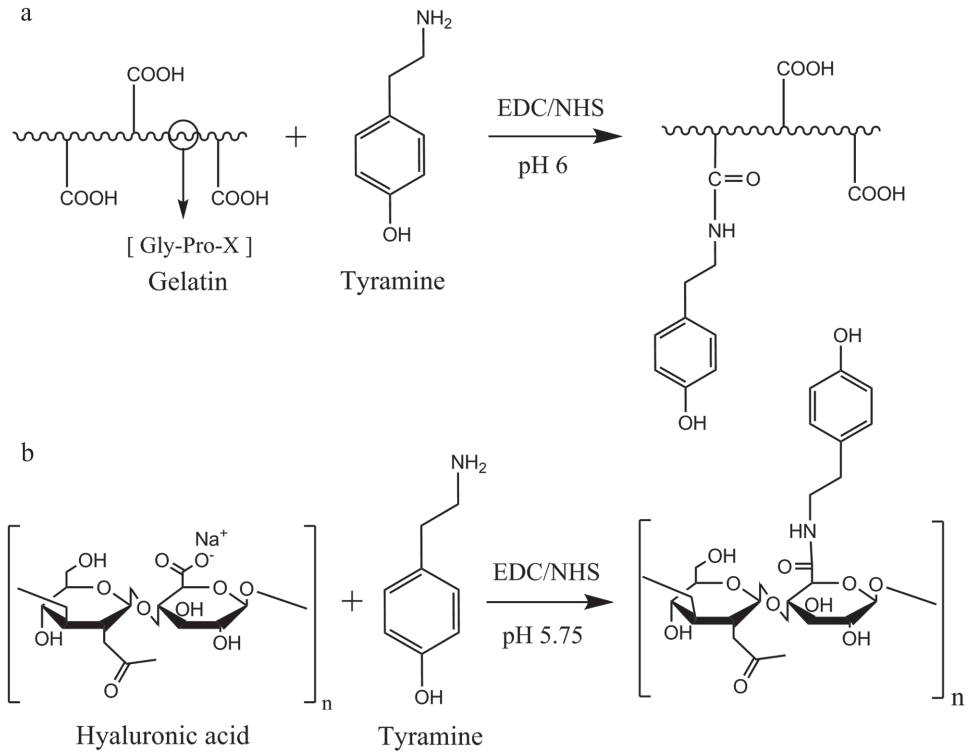

Figure 1. Tyramine grafting in a) gelatin and b) hyaluronic acid polymeric chains.

swept for 20 min at 37 °C and samples gelation took place during that time. The stabilization time of the storage modulus was used to compare the gelation dynamics of our hybrid gels as this is an important parameter in the hydrogel implantation process. As can be seen in Figure 3, the fastest stabilization time is for pure Gel (100/0), while for HA is the slowest. When Gel is present in a hybrid hydrogel composition, G'(t) is found to change rapidly in short times, but less so in longer times. By the end of the measurement, the storage modulus of pure Gel is totally stabilized, while a small but nonzero slope is observed in G′ for every hybrid gel and pure HA. The dependence of the slope $\frac{dG'(t)}{dt}$ on reaction time was calculated and the stabilization time was calculated as the cross-point of the initial and final slope. The fastest dynamics was observed in pure Gel, and stabilization time is longer when the HA ratio is increased in the hybrids (see Table 2).

3.1. SEM Images and Equilibrium Water Content

Figure 4a shows the microscopic morphology of the hydrogels with different Gel/HA compositions. As the images correspond to lyophilized samples, the different structures seen in the pictures are probably due to their different degrees of swelling and probably not to their different intrinsic network structures. The pores seen in the pictures should correspond to free water domains in the hydrogels plus additional artifacts that could be introduced when freezing the samples previously to their lyophilizaton. Hydrogel pore size increases with higher HA content (see Table 2). The statistical analysis shows two well differentiated groups, one formed by 100/0, 70/30, and 50/50 Gel/HA hydrogels, with no significant statistical differences in average pore size of around 17 μm. The other group is formed by 30/70 and 0/100 Gel/HA, which have larger pore size (26 and 37 μm, respectively). Both show statistically significant differences with the higher Gel content group.

The quantity of DPBS absorbed by the different Gel/HA compositions was measured as previously described and the obtained values can be seen in Figure 4b. The amount of water within the hydrogels increases with higher quantities of HA in the hydrogel composition. This higher water content causes the larger pore size seen in the SEM images.

An EWC of 2924% for Gel and 8790% for HA were obtained, the different mixtures having intermediate values (see Table 2). The statistical analysis indicates significant differences (see Figure 4b) between all the samples except between the 70/30 and 50/50 hydrogels.

Raising the HA content increases the quantity of water that the hydrogels are able to absorb and consequently the pore size. This higher expansion of HA, or the mixtures rich in HA, is traduced into a higher volumetric ratio, which is a more visual magnitude (also included

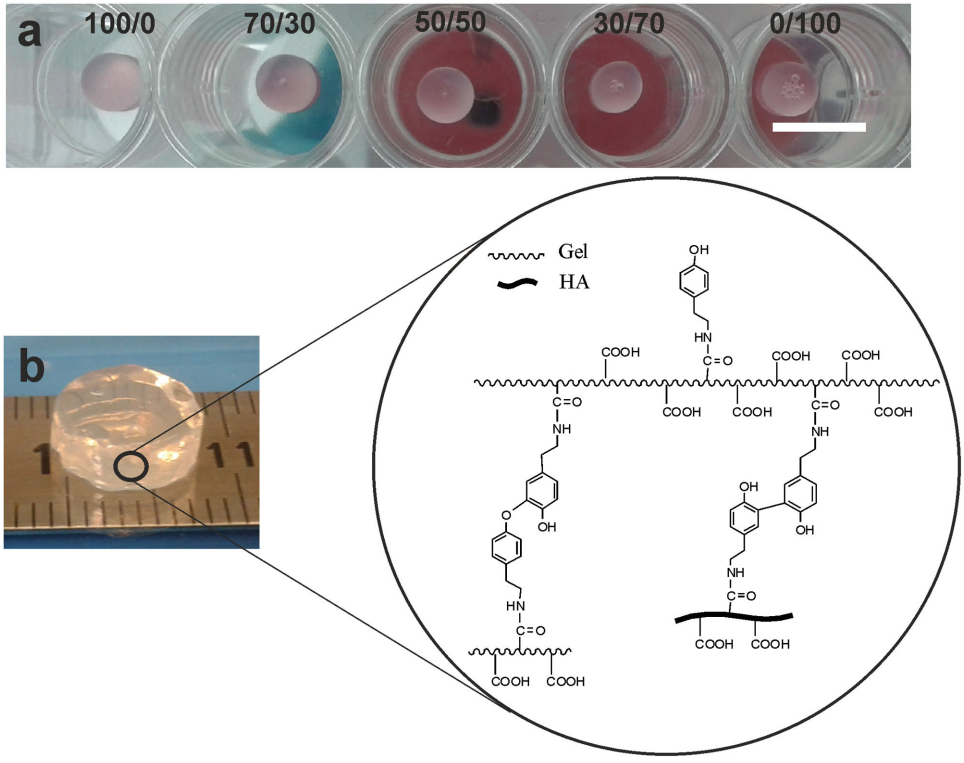

Figure 2. a) Macroscopic image of Gel/HA hydrogels used in cell culture experiments, 50 µL hydrogels were prepared for each composition, and the pictures correspond to the samples with encapsulated cells prior to add the cell culture medium, and b) macroscopic image of 70/30 Gel/HA hydrogel used for EWC and mechanical experiments. The molecular structure obtained after enzymatic crosslinking with HRP/H_2O_2 between Gel and HA tyramine grafted chains is shown. Scale bar is 1 cm.

in Table 2). While HA hydrogel has a volume in equilibrium that is almost 12 times that of the dry polymer, Gel hydrogel volume is only 5 times higher than that of dry Gel, being the mixtures between these values. This higher water retention in HA is explained mainly by its hygroscopic nature, obtaining hydrogels with a larger pore size when the percentage of HA increases,[23] and/or less crosslinking,[24] in this case by reduced tyramine grafting, which would lead to a greater distance between crosslinking points and more space to lodge water within its polymeric structure.[24]

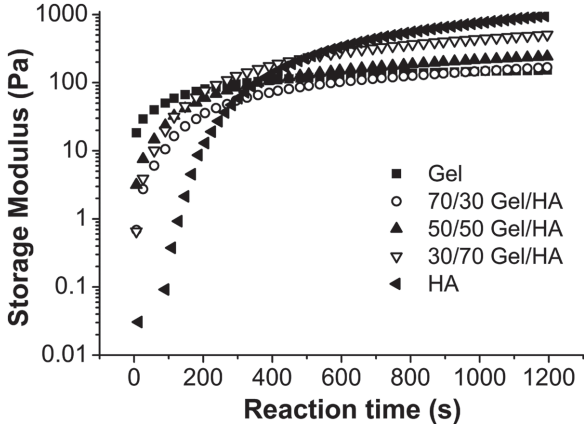

Figure 3. Crosslinking kinetics at 37 °C represented with storage modulus as a function of reaction time at a frequency of 1 Hz and 1% strain. Each curve corresponds to the average of three different samples.

Equilibrium swelling results can be used to estimate the apparent crosslinking density of the different hydrogel networks (ρ_x) through a very simplified model of the Flory–Rehner equation:[25]

$$\rho_x = -\frac{\ln\varphi_w + (1-\varphi_w) + \chi\cdot(1-\varphi_w)^2}{v_w\left[(1-\varphi_w)^{1/3} - (1-\varphi_w)/2\right]} \quad (4)$$

where φ_w is the volume fraction of water in the swollen state, χ the polymer–water interaction parameter and v_w the molar volume of water. Interaction parameter values were taken from the literature, χ = 0.49 for Gel[19] and χ = 0.473 for HA,[20] considering ideal behavior for the mixtures. Crosslinking density is related with the average molecular weight between crosslinks in the networks $M_c = \rho_{polymer}/\rho_x$ that was also estimated. Both parameters were listed in Table 2 for the different hydrogels. These values are considered approximations but can be useful to have an idea of the different network structures. As seen in Table 2, Gel has a higher crosslinking density (and lower average molecular weight between crosslinks)

Table 2. Properties of the different Gel/HA hydrogels (gelation time estimated from the time evolution of the storage modulus (Figure 3) in the rheometer, pore size, EWC, volumetric swelling ratio (Q_v), crosslinking density, and mean molecular weight between crosslinks (M_c)).

Gel/HA hydrogel	Gelation time [min]	Pore size [μm]	EWC [%]	Q_v	Crosslinking density [mol m^{-3}]	M_c [g mol^{-1}]
100/0	1.87 ± 0.23	18.2 ± 2.9	2924 ± 169	43.1 ± 3.4	1.95	737648
70/30	2.25 ± 0.15	16.2 ± 3.6	4597 ± 489	64.0 ± 7.7	1.14	1199010
50/50	2.19 ± 0.23	17.4 ± 5.6	5232 ± 620	70.4 ± 9.2	1.11	1193743
30/70	2.41 ± 0.07	25.9 ± 12.5	6390 ± 439	83.1 ± 6.6	0.93	1375407
0/100	4.54 ± 0.08	37.2 ± 8.9	8790 ± 1363	109.0 ± 17.7	0.69	1790180

than HA, which is consistent with the higher substitution degree of the GEL–Tyr. The crosslinking densities for the mixtures are within the Gel and HA values.

3.2. Compression Tests

E values of muscle are in the range of 8–17 kPa.[26] The pure HA hydrogel has a Young's modulus in the same order of magnitude as muscle but lacks cell adhesion sequences. To compensate for this, Gel was incorporated into the system, which in turn modifies its mechanical properties. Changes in the mechanical characteristics of the polymeric network can influence the cell traction forces exerted on it, as it is easier for cells to contract softer matrices.

Unconfined compression tests in immersion were performed on the different Gel/HA samples. A representative stress-strain curve for each composition was selected in order to better understand the hydrogel behavior (see Figure 5a). A linear behavior can be seen in all the samples at up to 30% strain. In this range water flows out of the hydrogel when compression forces are increased. After this point, the slope gradually changes and the hydrogel water content is probably reduced, with the mechanical properties of the polymeric matrix being more noticeable. The depicted curves show that for hydrogels with a higher HA content, higher stress or force is needed to deform the material at a given strain.

The compressive Young's moduli for the samples immersed in DPBS are given in Figure 5b and Table 3, calculated from the initial linear region of the stress-strain curves at up to 20% strain. Higher HA content in the Gel/HA mixtures increases the compressive strength of the hydrogels and higher Young's moduli were obtained. A value of 4 kPa versus 6.9 kPa was calculated for pure Gel and HA, respectively, the different Gel/HA hydrogels having intermediate values. The highest Young's modulus obtained in the Gel/HA hybrids was for 30/70 Gel/HA with 5.5 kPa. Significant differences were obtained between 0/100 Gel/HA and all the other groups and between 100/0 Gel/HA with 50/50 and 30/70 Gel/HA.

Several factors contribute to the mechanical stiffness of hydrogels: the molecular weight between crosslinks or crosslinking degree, the water content, the chemical composition, the rigidity

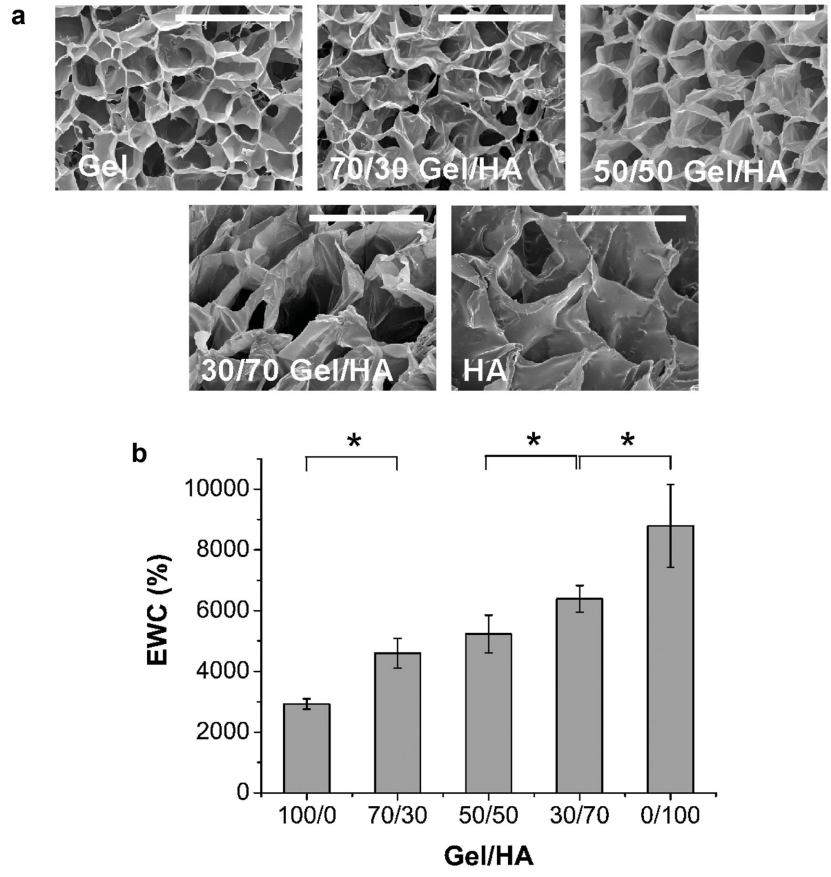

Figure 4. a) Scanning electron microscope images of the five different Gel/HA hydrogels. Scale bar corresponds to 60 μm. b) Equilibrium water content of the different Gel/HA compositions in DPBS at 37 °C. * indicates statistical significance between groups.

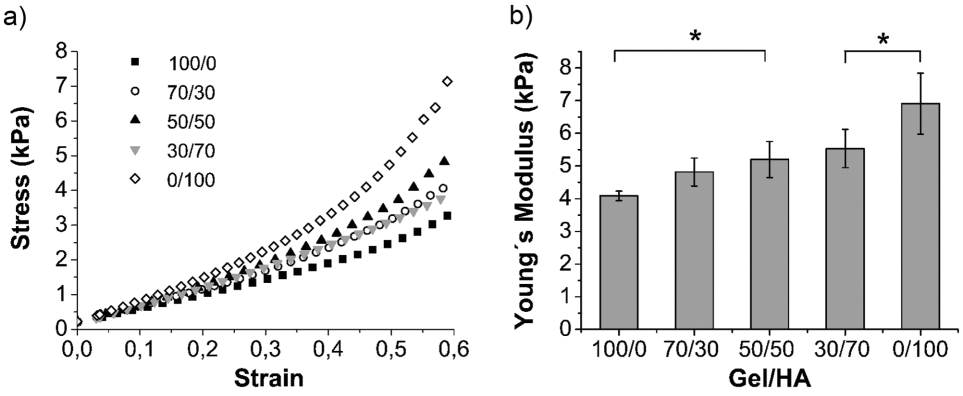

Figure 5. a) Stress versus strain curves of the Gel/HA hydrogels under compression and b) Young's modulus from 0 to 20% strain of the samples immersed in DPBS, $n = 5$. * indicates statistical significance between groups.

of the chains, and the water permeability coefficient. Gel has a higher crosslinking degree and lower molecular weight between crosslinks than HA network, which is consistent with the higher degree of tyramine substitution and lower water content [see Table 2]. Based on these parameters, Gel hydrogel should have a higher stiffness and Young's modulus than HA, which is just opposite to what the mechanical experiments demonstrate. HA has been reported to be a very rigid chain in water, what can be one cause of its higher stiffness.[27] Besides that, and in a similar way as occurs in soft hydrated tissues like cartilage, the mechanical resistance of hydrogels at low deformations can be governed by the water retained in their structure when deforming, which acts as an incompressible fluid resisting compressibility forces.[28] Reported values of hydraulic permeability for HA are quite lower than for Gel (or collagen), $1.8–1.9\times10^{-12}$ m^4 $N^{-1}\cdot s^{-1}$[29] and 0.758×10^{-10} m^4 $N^{-1}\cdot s^{-1}$,[30] respectively (both for 1% hydrogels). This resistance of water to flow from the HA network when deforming can be also a cause of its higher Young's modulus. For the same reasons, the Young's modulus increases as the ratio of HA in the different mixtures does.

The typical Young's moduli (E) values of natural hydrogels are in the order of magnitude of a few kPa.[31] In this study, we obtained hydrogels with E values ranging from 4 to 7 kPa (see Table 3). In another study with enzymatically crosslinked HA–Tyr hydrogels, Lee et al. found that the increase in H_2O_2 concentration produced an increase in its storage modulus, which has been correlated with the higher crosslinking density of the hydrogel when higher oxidation is achieved by the H_2O_2.[21] The reaction mechanism produced by the HRP/H_2O_2 coupling starts with the oxidation of the HRP by the H_2O_2, which afterward oxidizes the tyramine groups of the HA or the Gel chain, see Figure 2b.[21] Then the percentage of tyramine groups forming crosslinking points will depend not only on the quantity of tyramine moieties grafted onto the Gel or HA backbone, but also on the amount of H_2O_2. In the above study, HA–Tyr hydrogels were obtained with a storage modulus of 3 kPa, this value being lower than the value obtained in the present study. This was partly due to the lower molecular weight of their HA (90 kDa compared to 300 kDa used here) and also to lower HRP and H_2O_2 concentrations.

Toh et al. also studied the effect of varying the H_2O_2 concentration from 500 to 1000×10^{-6} M and obtained a compressive Young's modulus from 5 to 11 kPa and a reduction of the swelling ratio (m_w/m_d) from 43 to 33, which confirms that higher H_2O_2 concentrations promote

Table 3. Mechanical properties and cell differentiation of the different Gel/HA compositions (compressive Young's modulus and myoblast differentiation).

Gel/HA hydrogel	Young's modulus [kPa]	Cell differentiation [%]	
		Periphery	Center
100/0	4.1 ± 0.1	48.8 ± 8.1	0 ± 0
70/30	4.8 ± 0.4	57.2 ± 5.2	35.3 ± 7.6
50/50	5.2 ± 0.5	54.5 ± 8.9	10.8 ± 5.7
30/70	5.5 ± 0.6	57.8 ± 5.5	26.9 ± 13.6
0/100	6.9 ± 0.9	0 ± 0	0 ± 0

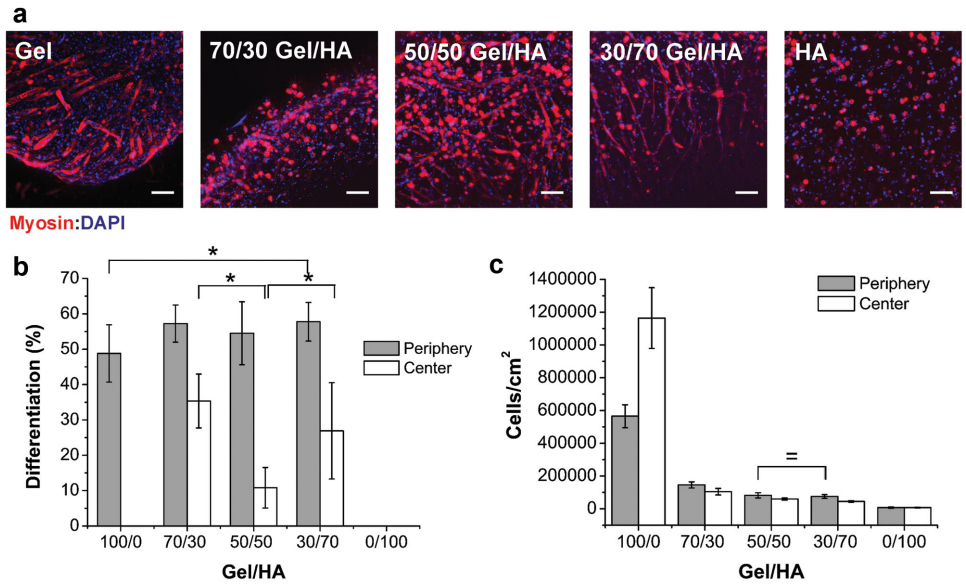

Figure 6. a) Differentiation of C2C12 cells, as indicated by sarcomeric myosin in Gel/HA hydrogels. Images were obtained as the *z* projections of images at different heights. Scale bar is 100 μm. b) Percentage of cell differentiation and c) total number of cells in the different hydrogel compositions. * and = symbols indicate statistical significance and no statistical significance between groups, respectively.

hydrogel crosslinking.[32] In this study, HRP and H_2O_2 concentrations were kept constant in order to observe the effect of the two hydrogel components, Gel and the HA.

Exhibiting the Gel/HA mixtures higher compressive strength than pure Gel they have the advantage over pure HA that they contain the RGD sequences for cell adhesion of Gel.[14,33] Incorporating the RGD sequence into different hydrogel matrices has been reported to induce myoblast adhesion, proliferation, and differentiation,[3a,c,6d] as well as to improve adhesion to other cell types.[3f,34]

3.3. Myogenic Differentiation

Figure 6a shows the *z* projections of stained sarcomeric myosin in the different Gel/HA compositions. Gel promoted myotube formation in all cases, whereas the cells in the HA hydrogel stayed round and no myotubes were formed.

Figure 6b and Table 3 show the percentage of cells expressing sarcomeric myosin (shown in the figure as percentage of differentiation). The results show higher expression at the periphery of the hydrogels, mainly due to higher nutrient availability.

Only isolated cells were observed in HA, which implies lack of cell differentiation and myotube organization. Cells located in the center of the hydrogel formed myotubes in the three Gel/HA mixtures analyzed. The high proliferation of cells in the Gel hydrogel and the substantial shrinkage of the hydrogel itself did not allow myotube formation in the interior of Gel hydrogels. This effect can be elucidated from Figure 5c, in which the quantity of cells per area is represented, showing a large number of cells at the center of the Gel hydrogel.

Figure 7 shows the cell morphology in the different Gel/HA hydrogels at high magnification. Expression of myosin was marked in red and formation of myotubes could be seen in all the compositions, except for the HA hydrogel.

Our results clearly show that cell differentiation happened mainly in the outer regions of the Gel hydrogel (Figure 6b), while the cell population was high at the center but no myosin expression was revealed. In 70/30, 50/50, and 30/70 Gel/HA hybrids, cells expressing myosin appeared throughout the entire hydrogel, although more myotubes were seen at the periphery, which were larger in the mixtures than in the Gel hydrogel (Figure 6a,b).

Anchorage-dependent cells need sufficient substrate stiffness able to resist forces generated by cells to properly activate cell response. Discher et al. have demonstrated that contractile cells as myoblasts have an optimal tissue-like matrix, which is stiff but at the same time compliant enough to balance cell adhesion, contractility, and ultimately promote cell differentiation.[35] They proved that when C2C12 cells were cultured for 2 weeks in very soft gels, with Young's modulus < 5 kPa, they expressed a very diffuse actin cytoskeleton and myosin staining. The same was found in very stiff gels or glass substrates with Young's modulus > 23 kPa. For two weeks of culture, gels with intermediate stiffness, between 8 and 11 kPa, showed adequate expression of actin and myosin and for four weeks of culture this occurred between 6.5 and 17 kPa. An optimum value of Young's modulus of ≈12 kPa was suggested in this work for myoblast differentiation.

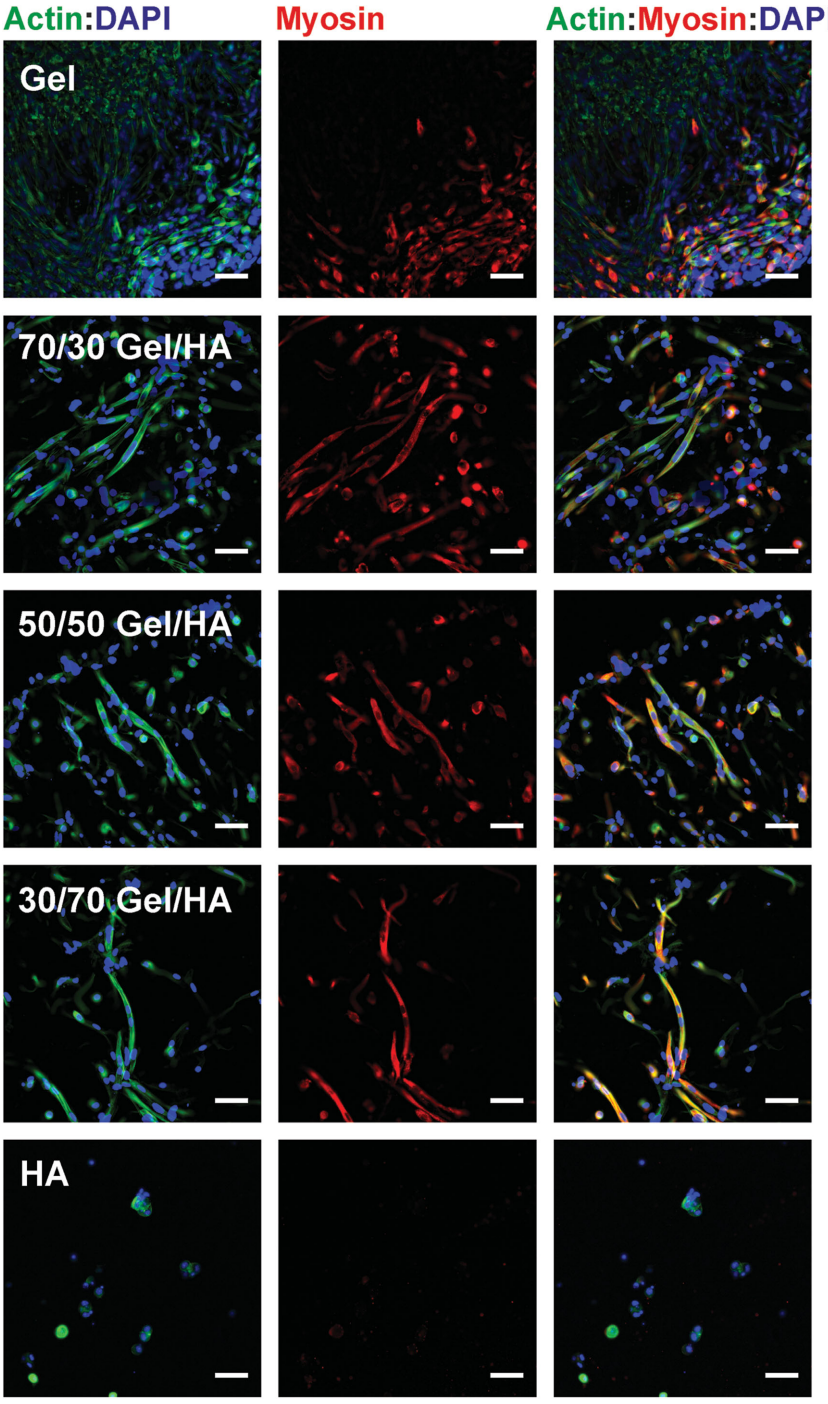

Figure 7. Differentiation of C2C12 cells in the different Gel/HA compositions after 4 d in differentiation media. Myosin, actin, and DAPI were stained in 40 μm hydrogel sections. Scale bar is 50 μm.

Similarly Kaji et al.[36] reported that collagen membranes with similar stiffness, Young's modulus of 14.8 ± 1.95 kPa, also induced myogenic differentiation of C2C12, proved by the sarcomeric structures found within the myotubes. Young's modulus of Gel, 4.1 ± 0.1 kPa (see Table 3), is in the range of what has been classified as very soft hydrogels. According to the literature, this value is not enough to promote C2C12 differentiation. For Gel, 49% differentiation was obtained at the hydrogel periphery but no differentiation occurred in the center due to hydrogel shrinkage, probably due to cell-matrix traction or contractile forces.[3c,37] Activation of cell contractility during myoblast differentiation was not counterbalanced by the stiffness of the gel, and resulted in the collapse of the material and the lack of cell differentiation. The importance of contractility in myogenesis has been previously reported in other material systems.[38] Other studies have reported this shrinkage in collagen hydrogels. Oh et al. seeded rat bone marrow mesenchymal stem cells (MSCs) in collagen hydrogels at different cell seeding densities (from 5×10^4 to 5×10^5 cells mL^{-1}) and reported hydrogel shrinkage at 3–4 weeks of cell culture for the hydrogel with the highest cell seeding.[39] Zhang et al. seeded 2, 10, and 50 million cells mL^{-1} (rabbit bone marrow MSCs) in Type II collagen hydrogels (7 mg mL^{-1}). After 7 d of culture 50–60% hydrogel contraction was obtained for the highest cell seeding density and slightly less at the other two cell densities. They also reported a plateau after cell proliferation at 7 d.[40] Gel hydrogel shrinkage thus seems to be related to the cell seeding density of the hydrogels and the strong forces that the cells exert on the surrounding matrix.

On the contrary, Young's modulus of the Gel/HA hybrids (Table 3) are in the range of what has been named muscle tissue-like stiffness that promotes myogenic differentiation.[35a,36] In Gel/HA mixtures, myotube formation could be seen throughout the entire hydrogel, although myoblast differentiation was higher at the periphery (see Table 3). Traction forces exerted by cells can be counterbalanced by the polymeric network due to the higher mechanical stiffness of these matrices, avoiding hydrogel shrinkage. In comparison, 35% differentiation was obtained in 70/30 Gel/HA, 11% in 50/50, and 27% in 30/70 at the center of the hydrogel, while there was no differentiation at the center in pure Gel and pure HA. Higher peripheral differentiation was

obtained in Gel/HA hybrids (58% for 30/70 Gel/HA) than in pure Gel (49% for 100/0 Gel/HA).

On the other hand, no myosin and no myotubes were formed in the HA hydrogel. Cells remained rounded inside the hydrogel and almost no proliferation was observed. As expected, the lack of adhesion sites in HA[34] prevented cell adhesion and rounded cells were seen to proliferate slowly and form clusters inside the gel, as previous studies on MSCs and neural precursor cells have reported.[41] Consequently no myotube formation was achieved. The same occurred in pure chitosan[3d] or alginate[42] hydrogels, polysaccharides similar to acid hyaluronic that does not support cell adhesion. There C2C12 adhesion, proliferation and differentiation only occurred in combination with the adhesive RGD sequence. However, despite the lack of adhesion to HA, increased cell seeding density might promote myoblast cell–cell contacts and then probably myotube formation,[43] this deserves further investigation which is beyond the scope of this work. No shrinkage was observed in HA hydrogels due to the lack of cell adhesion and hydrogel stiffness. Other cells able to interact with HA through their CD44 receptor, e.g., MSCs, yield hydrogel contraction specially for reduced cross-linking grades.[32]

The Gel/HA hybrids showed better properties than their pure components in allowing myotube formation and being good candidates for skeletal muscle tissue engineering. As 30/70 Gel/HA hydrogel promoted myoblast differentiation and at the same time was the mixture with higher stiffness it would be proposed as the most suitable hybrid for myoblast differentiation.

3.4. Effect of a Cell Contractility Inhibitor

At the cell seeding density used (8×10^6 cells mL^{-1}), C2C12 cells considerably contracted the Gel matrix and a very small hydrogel remained after the cell culture. Although it is known that the contractile mechanism must be activated for C2C12 differentiation into myoblasts,[44] this needs to be counterbalanced by the ECM's mechanical properties to be effective. As we wanted to test whether the gel shrinkage was actually a consequence of cell contractility, we studied differentiation using blebbistatin cell contractility inhibitor in the hydrogels with higher Gel content (100/0 and 70/30 Gel/HA).

Results in Figure 8 reveal the specific effect of cell contractility in gel shrinkage and cell differentiation. Immunofluorescence images of 100/0 and 70/30 Gel/HA cultured in the presence of blebbistatin can be seen in Figure 8a. A higher level of hydrogel contraction was obtained in the pure Gel hydrogel than in 70/30 Gel/HA (Figure 8b), due to the higher Gel content and the fact that myoblasts have fewer adhesion sequences. Moreover, the presence of blebbistatin in the cell culture medium reduced hydrogel contraction in both types. After 4 d,

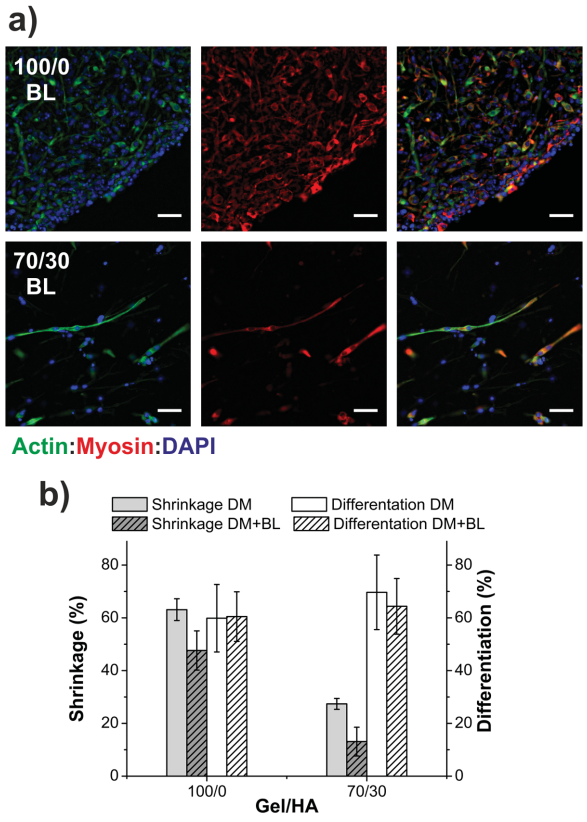

Figure 8. a) C2C12 differentiation in 100/0 and 70/30 Gel/HA hydrogels in the presence of blebbistatin (a contractility inhibitor, BL). b) Shrinkage and percentage of differentiation for 100/0 Gel/HA and 70/30 Gel/HA in differentiation medium (DM) and in medium with blebbistatin (DM+BL) after 4 d of culture. Scale bar is 50 μm.

100/0 Gel/HA had shrunk 63% in a normal differentiation medium, whereas shrinkage was 48% in the sample cultured with blebbistatin. In the case of 70/30 Gel/HA the shrinkage decrease was more marked as it dropped to half in the presence of blebbistatin, 27% in the differentiation medium and 13% with the contractility inhibitor. Both 100/0 and 70/30 Gel/HA compositions show less shrinkage when the culture was made with the cell contractility inhibitor, which shows the effect of cell contractility on the Gel matrix. Adding blebbistatin to the culture reduces gel shrinkage, keeping the level of differentiation unaffected (Figure 8b). This means that still with this reduced ability to perform force, Gel is too soft to counterbalance mechanical actions. On the other hand, the system Gel/HA 70/30 with already low level of shrinkage is mechanically less stressed after adding blebbistattn but cells still attain basically the same level of differentiation. Note that we have quantified the level of differentiation on the surface of the gel, which guarantees the availability of the inhibitor to cells. Note also that the level of differentiation remains unaffected as cell contractility is reduced only moderately due to the concentration of

inhibitor added, which maintains cell viability. Gel stiffness is too low and so diminishing cell contractility does not involve any change in cell differentiation. On the other hand, Gel/HA 70/30 has a modulus of ≈5 kPa and the reduction in contractility does not dramatically alter the ability of cells to deform an already soft gel.

To sum up, the combination of Gel/HA at different ratios, has an influence on: (i) the quantity of RGD sequences in relation to the quantity of Gel; (ii) the quantity of water in the hydrogel; higher HA content increases water retention; (iii) the mechanical properties; higher Young's modulus is obtained with the higher HA; and (iv) the ability of cells to upregulate contractility.

4. Conclusions

A series of Gel/HA (100/0, 70/30, 50/50, 30/70, and 0/100 vol/vol) injectable hydrogels were synthesized and the proportions of both components were varied in order to study the effects on their material properties and C2C12 cell differentiation. The presence of higher HA content in the hydrogel composition was found to yield higher Young's moduli and higher EWC. HA networks have lower crosslinking density and can lodge a higher quantity of water. The intrinsic rigidity of HA chains and the lower water permeability are probably the causes of the higher Young's modulus at compression. As we had hypothesized, C2C12 cells interact better with pure Gel hydrogel due to the presence of RGD adhesion sequences. Gel is a very soft hydrogel and the traction forces exerted by cells cannot be counterbalanced causing significant hydrogel shrinkage and inhibiting myoblast differentiation in the center of the sample. No myoblast differentiation was achieved in pure HA hydrogel due to the lack of cell adhesion to the matrix. For all the Gel/HA combinations, when both Gel and HA were present, myotube formation was achieved throughout the entire hydrogel and no shrinkage occurred, which indicates that these systems are good candidates for further skeletal muscle or soft tissue engineering studies.

Supporting Information

Supporting Information is available from the Wiley Online Library or from the author.

Acknowledgements: The authors are grateful for the financial support received from the Spanish Ministry through the MAT2013-46467-C4-1-R project (including the FEDER financial support), the BES-2011-046144, and the EEBB-I-14-08725 grants. CIBER-BBN is an initiative funded by the VI National R&D&I Plan 2008–2011, Iniciativa Ingenio 2010, Consolider Program. CIBER actions are financed by the Instituto de Salud Carlos III with assistance from the European Regional Development Fund. M.S.S. acknowledges ERC through HealInSynergy 306990.

Received: December 30, 2015; Revised: March 29, 2016; Published online: May 23, 2016; DOI: 10.1002/mabi.201500469

Keywords: gelatin; hyaluronic acid; injectable hydrogels; matrix stiffness; myoblast differentiation

[1] a) Y. Li, J. Rodrigues, H. Tomás, *Chem. Soc. Rev.* **2012**, *41*, 2193; b) G. D. Nicodemus, S. J. Bryant, *Tissue Eng., Part B* **2008**, *14*, 149.
[2] a) C. Frantz, K. M. Stewart, V. M. Weaver, *J. Cell Sci.* **2010**, *123*, 4195; b) C. Bonnans, J. Chou, Z. Werb, *Nat. Rev. Mol. Cell Biol.* **2014**, *15*, 786; c) J. K. Mouw, G. Ou, V. M. Weaver, *Nat. Rev. Mol. Cell Biol.* **2014**, *15*, 771.
[3] a) J. A. Rowley, D. J. Mooney, *J. Biomed. Mater. Res.* **2002**, *60*, 217; b) J. Kim, Y. Park, G. Tae, K. B. Lee, C. M. Hwang, S. J. Hwang, I. S. Kim, I. Noh, K. Sun, *J. Biomed. Mater. Res., Part A* **2009**, *88*, 967; c) A. S. Salimath, A. J. García, *J. Tissue Eng. Regener. Med.* **2014**, DOI: 10.1002/term.1881; d) Y. Yeo, W. Geng, T. Ito, D. S. Kohane, J. A. Burdick, M. Radisic, *J. Biomed. Mater. Res., Part B* **2007**, *81*, 312; e) I. Jun, S. J. Kim, E. Choi, K. M. Park, T. Rhim, J. Park, K. D. Park, H. Shin, *Macromol. Biosci.* **2012**, *12*, 1502; f) I. M. Chung, N. O. Enemchukwu, S. D. Khaja, N. Murthy, A. Mantalaris, A. J. García, *Biomaterials* **2008**, *29*, 2637.
[4] a) S. Distantina, R. Rochmadi, M. Fahrurrozi, W. Wiratni, *Eng. J.* **2013**, *17*, 57; b) B. V Slaughter, S. S. Khurshid, O. Z. Fisher, A. Khademhosseini, N. A. Peppas, *Adv. Mater.* **2009**, *21*, 3307; c) M. D. Brigham, A. Bick, E. Lo, A. Bendali, J. A. Burdick, A. Khademhosseini, *Tissue Eng., Part A* **2009**, *15*, 1645; d) M. N. Collins, C. Birkinshaw, *J. Appl. Polym. Sci.* **2007**, *104*, 3183.
[5] J.-Y. Lai, *J. Mater. Sci. Mater. Med.* **2010**, *21*, 1899.
[6] a) L. S. M. Teixeira, J. Feijen, C. A. van Blitterswijk, P. J. Dijkstra, M. Karperien, *Biomaterials* **2012**, *33*, 1281; b) S. Poveda-Reyes, L. R. Mellera-Oglialoro, R. Martínez-Haya, T. C. Gamboa-Martínez, J. L. Gómez Ribelles, G. Gallego Ferrer, *Macromol. Mater. Eng.* **2015**, *300*, 977; c) S. Sakai, K. Hirose, K. Taguchi, Y. Ogushi, K. Kawakami, *Biomaterials* **2009**, *30*, 3371; d) I. Jun, K. M. Park, D. Y. Lee, K. D. Park, H. Shin, *Macromol. Res.* **2011**, *19*, 911.
[7] V. Andrés, K. Walsh, *J. Cell Biol.* **1996**, *132*, 657.
[8] S. Gupta, T. Greeshma, B. Basu, S. Goswami, A. Sinha, *J. Biomed. Mater. Res., Part B* **2013**, *101B*, 346.
[9] D. Mawad, E. Stewart, D. L. Officer, T. Romeo, P. Wagner, K. Wagner, G. G. Wallace, *Adv. Funct. Mater.* **2012**, *22*, 2692.
[10] S. T. Cooper, A. L. Maxwell, E. Kizana, M. Ghoddusi, E. C. Hardeman, I. E. Alexander, D. G. Allen, K. N. North, *Cell Motil. Cytoskeleton* **2004**, *58*, 200.
[11] S. Ostrovidov, S. Ahadian, J. Ramon-Azcon, V. Hosseini, T. Fujie, S. P. Parthiban, H. Shiku, T. Matsue, H. Kaji, M. Ramalingam, H. Bae, A. Khademhosseini, *J. Tissue Eng. Regener. Med.* **2014**. DOI: 10.1002/term.1956.
[12] a) K. Nagamine, T. Kawashima, T. Ishibashi, H. Kaji, M. Kanzaki, M. Nishizawa, *Biotechnol. Bioeng.* **2010**, *105*, 1161; b) J. Ramón-Azcón, S. Ahadian, R. Obregón, G. Camci-Unal, S. Ostrovidov, V. Hosseini, H. Kaji, K. Ino, H. Shiku, A. Khademhosseini, T. Matsue, *Lab Chip* **2012**, *12*, 2959.
[13] S. Ostrovidov, X. Shi, L. Zhang, X. Liang, S. B. Kim, T. Fujie, M. Ramalingam, M. Chen, K. Nakajima, F. Al-Hazmi, H. Bae, A. Memic, A. Khademhosseini, *Biomaterials* **2014**, *35*, 6268.
[14] C. N. Grover, J. H. Gwynne, N. Pugh, S. Hamaia, R. W. Farndale, S. M. Best, R. E. Cameron, *Acta Biomater.* **2012**, *8*, 3080.

[15] G. Camci-Unal, D. Cuttica, N. Annabi, D. Demarchi, A. Khademhosseini, *Biomacromolecules* **2013**, *14*, 1085.
[16] X. W. Li, X. Y. Liu, N. Zhang, X. J. Wen, *J. Neurotrauma* **2014**, *31*, 1431.
[17] J. B. Rose, S. Pacelli, A. J. El Haj, H. S. Dua, A. Hopkinson, L. J. White, F. R. A. J. Rose, *Materials* **2014**, *7*, 3106.
[18] X. Z. Shu, Y. Liu, Y. Luo, M. C. Roberts, G. D. Prestwich, *Biomacromolecules* **2002**, *3*, 1304.
[19] H. B. Bohidar, *Int. J. Biol. Macromol.* **1998**, *23*, 1.
[20] J. B. Leach, K. A. Bivens, C. W. Patrick, C. E. Schmidt, *Biotechnol. Bioeng.* **2003**, *82*, 578.
[21] F. Lee, J. E. Chung, M. Kurisawa, *J. Controlled Release* **2009**, *134*, 186.
[22] J. L. Vanderhooft, M. Alcoutlabi, J. J. Magda, G. D. Prestwich, *Macromol. Biosci.* **2009**, *9*, 20.
[23] a) Y. S. Choi, S. R. Hong, Y. M. Lee, K. W. Song, M. H. Park, Y. S. Nam, *J. Biomed. Mater. Res.* **1999**, *48*, 631; b) Z. Zhou, Z. Yang, L. Kong, L. Liu, Q. Liu, Y. Zhao, W. Zeng, Q. Yi, D. Cao, *J. Macromol. Sci., Part B: Phys.* **2012**, *51*, 2392.
[24] X. Z. Shu, Y. Liu, F. Palumbo, G. D. Prestwich, *Biomaterials* **2003**, *24*, 3825.
[25] a) J. F. Martucci, R. A. Ruseckaite, A. Vazquez, *Mater. Sci. Eng., A* **2006**, *435–436*, 681; b) M. Monleon Pradas, J. L. Gomez Ribelles, A. Serrano Aroca, G. Gallego Ferrer, J. Suay Anton, P. Pissis, *Colloid Polym. Sci.* **2001**, *279*, 323.
[26] A. J. Engler, S. Sen, H. L. Sweeney, D. E. Discher, *Cell* **2006**, *126*, 677.
[27] B. J. Kvam, M. Atzori, R. Toffanin, S. Paoletti, F. Biviano, *Carbohydr. Res.* **1992**, *230*, 1.
[28] S. Kalyanam, R. D. Yapp, M. F. Insana, *J. Biomech. Eng.* **2009**, *131*, 081005.
[29] I. E. Erickson, A. H. Huang, S. Sengupta, S. Kestle, J. A. Burdick, R. L. Mauck, *Osteoarthritis Cartilage* **2009**, *17*, 1639.
[30] C. M. Tierney, M. G. Haugh, J. Liedl, F. Mulcahy, B. Hayes, F. J. O'Brien, *J. Mech. Behav. Biomed. Mater.* **2009**, *2*, 202.
[31] a) W. Y. Gu, H. Yao, C. Y. Huang, H. S. Cheung, *J. Biomech* **2003**, *36*, 593; b) H. Tan, C. R. Chu, K. A. Payne, K. G. Marra, *Biomaterials* **2009**, *30*, 2499; c) S. Bhat, A. Tripathi, A. Kumar, *J. R. Soc., Interface* **2011**, *8*, 540.
[32] W. S. Toh, T. C. Lim, M. Kurisawa, M. Spector, *Biomaterials* **2012**, *33*, 3835.
[33] B. Sarker, R. Singh, R. Silva, J. A. Roether, J. Kaschta, R. Detsch, D. W. Schubert, I. Cicha, A. R. Boccaccini, *PLoS One* **2014**, *9*, e107952.
[34] Y. Lei, S. Gojgini, J. Lam, T. Segura, *Biomaterials* **2011**, *32*, 39.
[35] a) A. J. Engler, M. A. Griffin, S. Sen, C. G. Bonnetnann, H. L. Sweeney, D. E. Discher, *J. Cell Biol.* **2004**, *166*, 877; b) M. A. Griffin, S. Sen, H. L. Sweeney, D. E. Discher, *J. Cell Sci.* **2004**, *117*, 5855.
[36] H. Kaji, T. Ishibashi, K. Nagamine, M. Kanzaki, M. Nishizawa, *Biomaterials* **2010**, *31*, 6981.
[37] a) A. Buxboim, I. L. Ivanovska, D. E. Discher, *J. Cell Sci.* **2010**, *123*, 297; b) A. D. Bershadsky, N. Q. Balaban, B. Geiger, *Annu. Rev. Cell Dev. Biol.* **2003**, *19*, 677; c) A. Oryan, S. Alidadi, A. Moshiri, N. Maffulli, *J. Orthop. Surg. Res.* **2014**, *9*, 18.
[38] M. Salmerón-Sánchez, P. Rico, D. Moratal, T. T. Lee, J. E. Schwarzbauer, A. J. García, *Biomaterials* **2011**, *32*, 2099.
[39] S.-A. Oh, H.-Y. Lee, J. H. Lee, T.-H. Kim, J.-H. Jang, H.-W. Kim, I. Wall, *Tissue Eng., Part A* **2012**, *18*, 1087.
[40] L. Zhang, T. Yuan, L. Guo, X. Zhang, *J. Biomed. Mater. Res., Part A* **2012**, *100A*, 2717.
[41] a) S. Sahoo, C. Chung, S. Khetan, J. A. Burdick, *Biomacromolecules* **2009**, *9*, 1088; b) L. Pan, Y. Ren, F. Cui, Q. Xu, *J. Neurosci. Res.* **2009**, *87*, 3207; c) T.-W. Wang, M. Spector, *Acta Biomater.* **2009**, *5*, 2371.
[42] J. L. Drury, T. Boontheekul, D. J. Mooney, *J. Biomech. Eng.* **2005**, *127*, 220.
[43] K. Tanaka, K. Sato, T. Yoshida, T. Fukuda, K. Hanamura, N. Kojima, T. Shirao, T. Yanagawa, H. Watanabe, *Muscle Nerve* **2011**, *44*, 968.
[44] a) S. B. P. Chargé, M. A. Rudnicki, *Physiol. Rev.* **2004**, *84*, 209; b) J. Dhawan, D. M. Helfman, *J. Cell Sci.* **2004**, *117*, 3735.